Inorganic Chemistry

Article

pubs.acs.org/IC

Triarylborane-Appended New Triad and Tetrad: Chromogenic and Fluorogenic Anion Recognition

Chinna Ayya Swamy P and Pakkirisamy Thilagar*

Department of Inorganic and Physical Chemistry, Indian Institute of Science, Bangalore 560012, India

Supporting Information

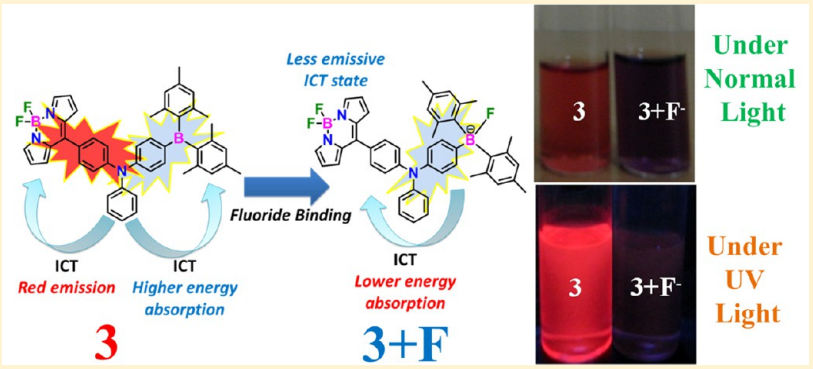

ABSTRACT: Facile synthesis of triad **3** and tetrad **4** incorporating $-B(Mes)_2$ (Mes = mesityl (2,4,6-trimethylphenyl)), boron dipyrromethene (BODIPY), and triphenylamine is reported. Introduction of two dissimilar acceptors (triarylborane and BODIPY) on a single donor resulted in two distinct intramolecular charge transfer processes (amine-to-borane and amine-to-BODIPY). The absorption and emission properties of the new triad and tetrad are highly dependent on individual building units. The nature of electronic communication among the individual fluorophore units has been comprehensively investigated and compared with building units. Compounds **3** and **4** showed chromogenic and fluorogenic responses for small anions such as fluoride and cyanide.

INTRODUCTION

Combinations are more versatile than individual entities. It is the combinations of genes that help life to evolve and move forward. Likewise in chemistry, combinations of elements produce molecules and versatile materials for various applications. Recently, combination of chromophores (multichromophoric assemblies) has received significant attention.[1] Suitably designed structures with precise energy/electron-transfer processes can efficiently mimic the natural energy harvesting process (photosynthesis).[2] On the other hand, if the structural building units are luminophores,[3] suitable manipulations of electronic communications between the building units can lead to materials that would find applications in organic light-emitting diodes (OLEDs),[3a,d,e,g,i,j] biological assays,[3h] and molecular recognition.[3b,c,f]

Recently, boron-containing luminophores such as boron dipyrromethene[4] (BODIPY) and triarylboranes[5] (TAB) have attracted much attention. Owing to their inherent Lewis acidity and notable solid-state fluorescence properties, TABs have found applications in optoelectronic devices,[4a−e,i] energy harvesting materials,[5l] and anion sensing.[5g,h,j] On the other hand, due to their excellent optical properties and structural flexibility, BODIPYs have found numerous applications in ion recognition,[4a,g,k] biological labeling, cell imaging,[4c−e,i] and dye-sensitized solar cells.[4a,j] In recent times, combinations of TAB and BODIPY have attracted considerable interest.[6] Recently we showed that compact dyad structures consisting TAB and BODIPY units were found to be "dual-emissive," with two distinct emission bands arising from the individual building units.[6f] Thus, a combination of the two different units in a compact fashion opens new avenues for accessing a range of new luminescent materials.

Our initial success with TAB and BODIPY combinations encouraged us to explore the molecular combinations containing more than two building units. In this regard $-B(Mes)_2$ (Mes = mesityl (2,4,6-trimethylphenyl))-, triphenylamine (TPA)-, and BODIPY-containing triad and tetrad have attracted our attention. Previous studies have shown that both TAB[7] and BODIPY[8] are electron deficient and exhibit intramolecular charge transfer (ICT) characteristics, if a suitable electron donor is attached. We reasoned that, if two structurally and optically distinct acceptors such as $-B(Mes)_2$ and BODIPY are attached to a single donor (TPA), such a combination would induce two dissimilar ICT processes (TPA to TAB and TPA to BODIPY) in different regions of the electronic spectrum. The energy difference between these two ICT processes may result in intriguing emission features upon photoexcitation at respective

Received: July 1, 2013
Published: March 4, 2014

   dx.doi.org/10.1021/ic402898n | *Inorg. Chem.* 2014, 53, 2776−2786

Scheme 1. Synthesis of 3 and 4. a = *n*-BuLi/THF (−78°C), Mes_2BF; b = THF/2N HCl; c = Pyrrole/CH_2Cl_2, $BF_3{\cdot}Et_2O$ (Catalytic) Followed by DDQ; Et_3N and $BF_3{\cdot}Et_2O$

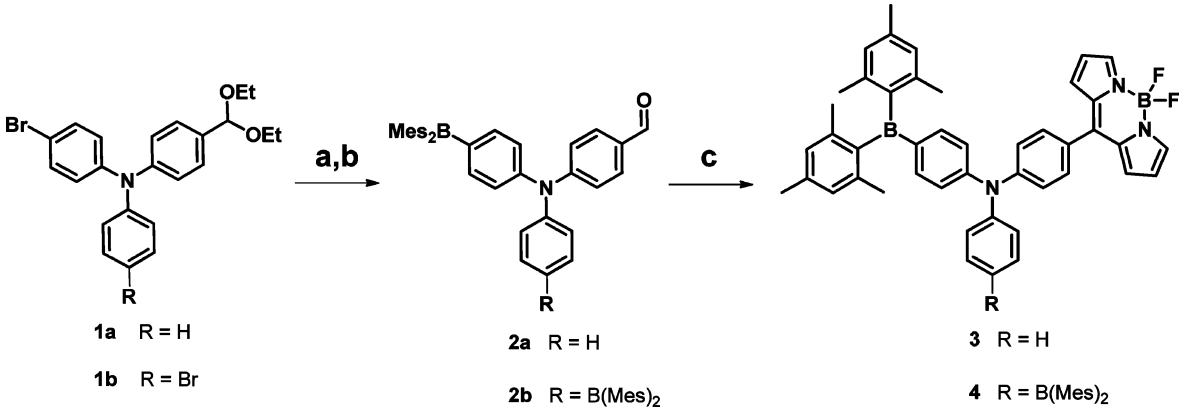

Chart 1. Structures of Model Compounds Used in This Study

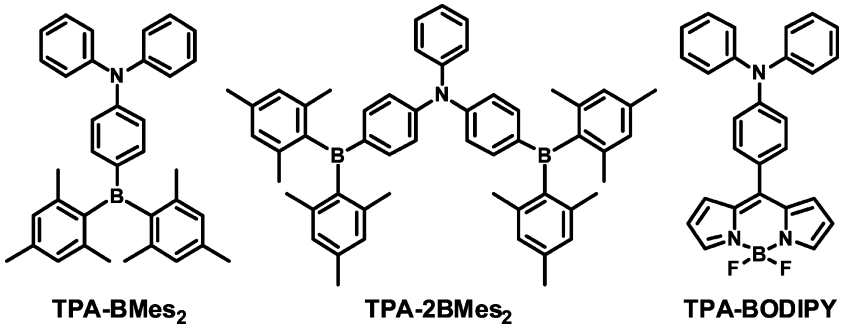

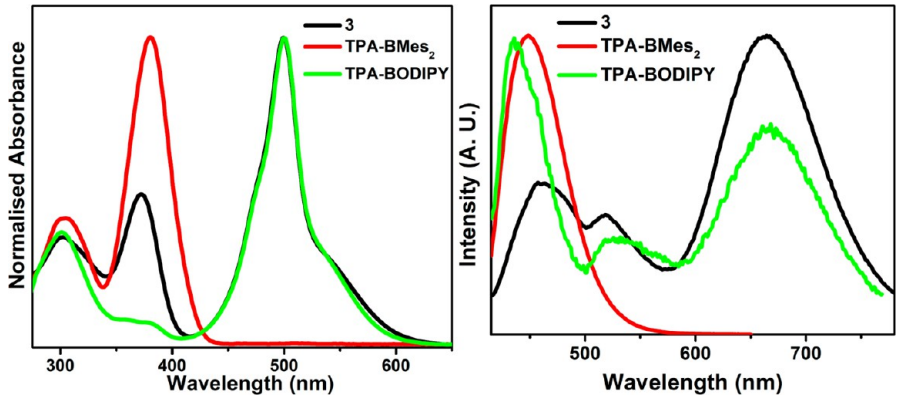

Figure 1. The normalized UV−vis (left) and emission spectra (λ_{ex} = 400 nm) (right) of **3** with model compounds $TPA\text{-}BMes_2$ and TPA-BODIPY in $CHCl_3$ (10 μM).

ICT bands. In addition, the presence of anion receptor $-B(Mes)_2$ will provide an opportunity to selectively control the ICT process by addition of a suitable nucleophile.[6f,7b] To rationalize our hypothesis, we designed and synthesized new triad **3** and tetrad **4**, incorporating $-B(Mes)_2$, BODIPY, and TPA units. The intriguing photophysical properties and their selective fluorogenic and chromogenic response toward smaller anions such as fluoride and cyanide are reported in this manuscript.

RESULTS AND DISCUSSIONS

Synthesis and Characterization. The synthetic protocols to access the target compounds **3** and **4** are shown in Scheme 1. Formylation of TPA followed by bromination and further protection of aldehyde group using triethyl-orthoformate gave compounds **1a** and **1b** in quantitative yields. Reaction of **1a** and **1b** with *n*-BuLi and trapping the anion generated with $(Mes)_2BF$ followed by acid hydrolysis (2N HCl) gave compounds **2a** and **2b**, respectively. Triad **3** and tetrad **4** were constructed by the acid-catalyzed condensation reaction between the pyrrole and respective aldehydes (**2a** for **3** and **2b** for **4**), followed by oxidation using 2,3-dichloro-5,6-dicyanobenzoquinone (DDQ) and subsequent addition of triethylamine and $BF_3{\cdot}Et_2O$. For comparative studies, building units $TPA\text{-}BMes_2$, $TPA\text{-}2BMes_2$, and TPA-BODIPY (Chart 1) were also synthesized according to known literature procedures.[7a,d,8b] All the compounds were characterized by NMR spectroscopy and mass spectrometry

dx.doi.org/10.1021/ic402898n | *Inorg. Chem.* 2014, 53, 2776−2786

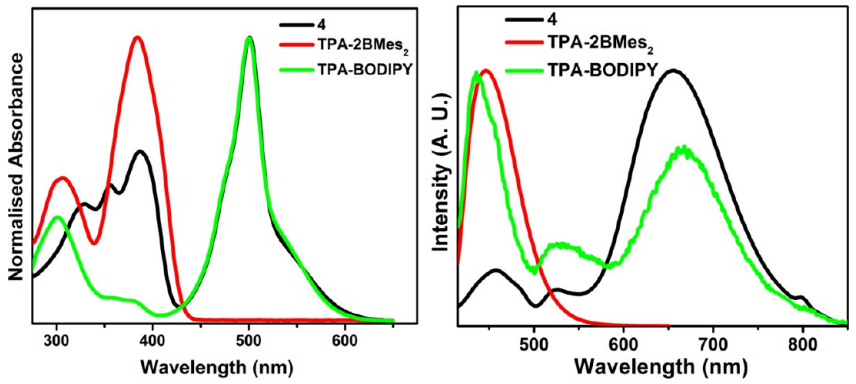

Figure 2. The normalized UV−vis (left) and emission spectra (λ_{ex} = 400 nm) (right) of **4** with model compounds TPA-2BMes$_2$ and TPA-BODIPY in $CHCl_3$ (10 μM).

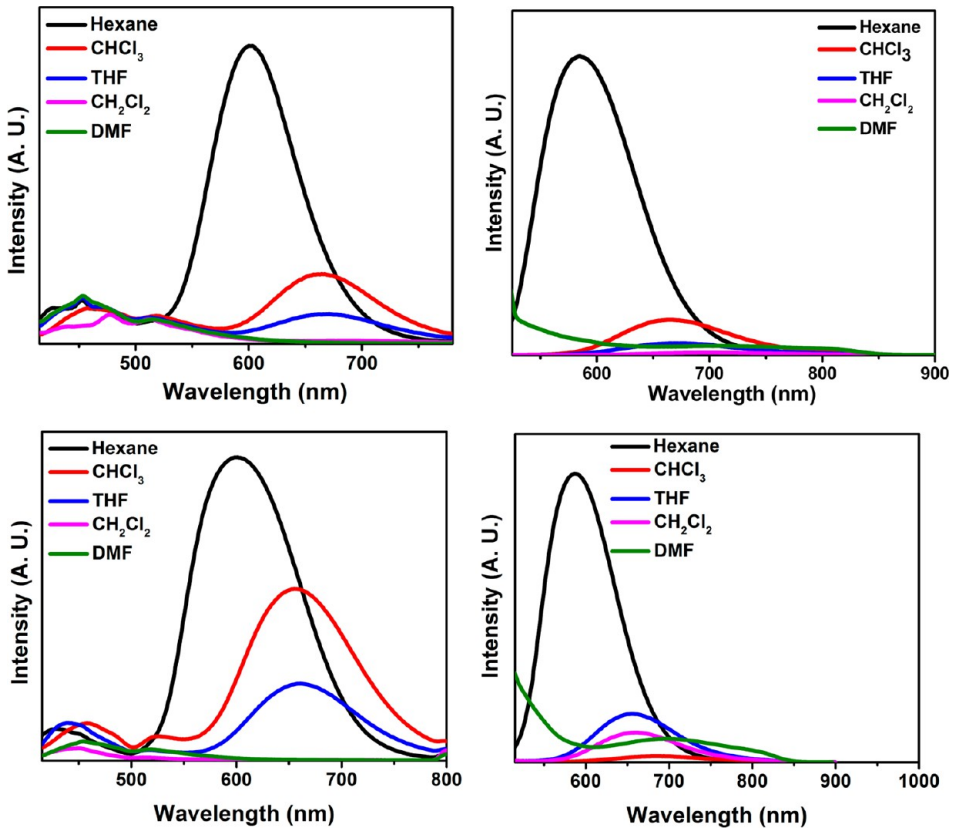

Figure 3. Fluorescence spectra of **3** (top left, λ_{ex} = 400 nm; top right, λ_{ex} = 500 nm) and **4** (bottom left, λ_{ex} = 400 nm; bottom right, λ_{ex} = 500 nm) in different solvents (10 μM).

(MS). The molecular structure of **4** was confirmed by single-crystal X-ray diffraction studies.

The ^{1}H NMR spectra of **3** and **4** are very similar. In particular, the pyrrole C−H resonances of indacene unit in **3** (6.57, 7.28, and 7.92 ppm) and **4** (6.57, 7.28, and 7.91 ppm) are close to each other. This indicates that the presence of additional boryl unit in **4** does not perturb the electronic nature of the indacene unit.

Photophysical Properties. Absorption profiles of compounds **3**, **4**, and the respective model compounds (TPA-BMes$_2$, TPA-2BMes$_2$, and TPA-BODIPY) are shown in Figures 1 and 2. The absorption spectrum of **3** as well as **4** is virtually the additive spectrum of the respective building units. Compounds **3** and **4** showed three major absorption events in the region 300 to 600 nm. Compound **4** shows more structured absorption in the higher energy region, when compared to **3**. Absorption peaks at ∼335 and ∼510 nm can be ascribed to the $\pi\rightarrow\pi^*$ transition centered at the TPA unit and the $S_0\rightarrow S_1$ transition of the BODIPY unit, respectively. The band at ∼380 nm and a weak shoulder at ∼550 nm are attributed to ICT from TPA to −B(Mes)$_2$ and from TPA to BODIPY, respectively. Compounds **3** and **4** show bands at ∼355 nm, which can be ascribed to the $\pi\rightarrow\pi^*$ transition involved in the TPA as well as triarylborane unit. These assignments are also in line with the observations reported by Mullen et. al.[7a,d] and Tang co-workers[8b] for TPA-BMes$_2$, TPA-2BMes$_2$, and TPA-BODIPY. As we envisioned vide-supra, the two electronically dissimilar acceptors −B(Mes)$_2$ and BODIPY induced two distinct ICT processes (∼380 nm and ∼550 nm) at different energy regions of absorption spectra of **3** and **4**. This result is completely different from the observations noted for TPA-2BMes$_2$.

dx.doi.org/10.1021/ic402898n | Inorg. Chem. 2014, 53, 2776−2786

Table 1. The Excited- and Ground-State Dipole Moments of Compounds 3 and 4

compounds	ground-state dipole moment (μ_g) (D)[a]	excited-state dipole moment (μ_e) (D)	$\mu_e - \mu_g$ (D)
3	6.77	41.04	34.27
4	5.91	40.31	34.40

[a]Ground-state dipole moment from DFT calculations.

Compounds **3** and **4** show similar fluorescence profiles (Figures 1 and 2). Triad **3** and tetrad **4** showed triple emission bands (~450, ~520, and ~660 nm) when excited in the region from 300 to 400 nm. The excitation at the BODIPY absorption region (480 to 570 nm) leads to a broad fluorescence band centered at 660 nm in nonpolar solvent such as hexane. Compounds **3** and **4** show no fluorescence upon excitation at the ICT absorption band (590 to 600 nm) (TPA to BODIPY) (see Figure 3). Concentration-dependent fluorescence studies and analysis of excitation spectra (the excitation spectra reproduce the respective absorption spectra, see Supporting Information, Figure S6) of respective fluorescence peaks suggest that the multiple emissions are only of intramolecular origin (Supporting Information). By comparing the fluorescence emission spectra of **3** and **4** with those of the respective building units (TPA-$BMes_2$ and TPA-BODIPY for **3**; TPA-$2BMes_2$ and TPA-BODIPY for **4**), one can assign the fluorescence bands at λ_{em} 450 and 520 nm as locally excited state (LE) emission from TPA-TAB and BODIPY units. The lower-energy emission peak at 660 nm can be ascribed to the emission from the excited state of the TPA-BODIPY ICT state. This ICT state can be populated by exciting the molecules either at TPA-TAB-centered or BODIPY-centered absorption band. Photoluminescence studies were carried out in solvents with different polarity. In polar solvents compounds **3** and **4** are nearly nonfluorescent. Only weak fluorescence bands were observed at 450 and 520 nm. Normally, the ICT states are stabilized in polar solvents due to their high dipole moment (μ_{ex} for **3** (41D) and **4** (40D), see Table 1 and Figure 4). In polar

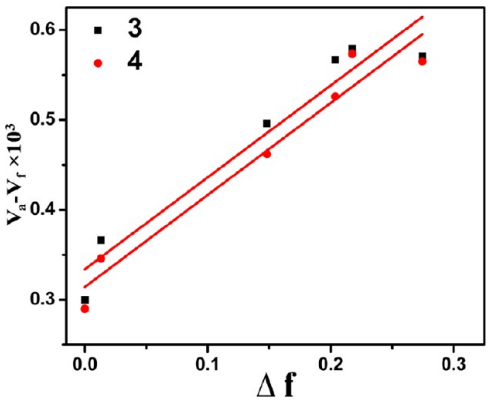

Figure 4. Lippert–Mattaga plots for **3** and **4** (see Supporting Information for equation)[8c,d]

environments the stabilization of ICT would lead to a charge-separated (CS) ionic state, which is nonfluorescent (as encountered in most of the instances)[9a,c,d] and quenches the emission from the ICT state. The weak emission feature observed in the higher-energy region (between 450 and 520 nm) is due to the LE state of TPA-TAB and BODIPY units. These assignments are also in line with the observations reported earlier.[8g–j] The excited-state dipole moments of **3** and **4** calculated from Lippert–Mattaga equation confirm the CT nature of the emissive species.

Anion Sensing Studies. Upon addition of fluoride as tetrabutylammonium fluoride salt (TBAF), both **3** (forming **3+F** with the fluoride anion) and **4** (forming **4+F** with the fluoride anion) showed similar changes in their absorption profiles. The peaks in the region of 300–400 nm disappeared gradually, and the intensity of the BODIPY absorption band decreased slightly with a blue shift of ~15 nm. Interestingly, a new $-Ar_3B-F-$TPA–BODIPY ICT band appeared and gradually gained in intensity at ~610 nm. Upon fluoride binding, the electron-deficient triarylborane moiety changes to an electron-rich borate moiety, and the resulting change in the electronic nature of the individual building units facilitates the fluoroborate (Ar_3B-F)-to-BODIPY ICT. The appearance of the new ICT band (~610 nm) is associated with a distinct color change (from orange to purple), which allows naked-eye detection of fluoride anion. Under similar conditions, addition of CN^- ion as tetrabutylammonium cyanide (TBACN) to **3** and **4** (giving **3+CN** and **4+CN**, respectively) showed changes in their absorption spectra similar to those observed for F^- binding, but the magnitude of changes is much smaller (see Figure 5). For example, even after addition of 10 equiv of CN^- to **3** and **4**, the absorption peaks in the region of 300–400 nm were quenched only partially. Although the new ICT band at ~610 nm could be observed, its intensity is significantly less compared to the ICT band observed for **3+F** and **4+F**. Addition of fluoride or cyanide ions to **3** and **4** quenches the emission peaks at ~660, 520, and 420 nm (λ_{ex} 400 nm, see Figure 6 and Table 2). Upon addition of 1.0 equiv of TBAF, compound **3** showed 75% quenching of fluorescence intensity, whereas **4** showed 83% decrease in intensity of ~660 bands upon addition 2.0 equiv of TBAF. To validate the role of solvents in the analyte selectivity, anion binding studies for compounds **3** and **4** were also carried out in tetrahydrofuran (THF) solutions (see Supporting Information). The observed spectral changes are similar to the spectra obtained for $CHCl_3$ solutions of **3** and **4**. Association constants were calculated (see Supporting Information, Table S1), and the results clearly indicate that the anion binding event is solvent-dependent. The association constants in THF solutions are higher than the values obtained in $CHCl_3$ solutions.[8m] This result is in accord with observations noted for triarylboranes reported elsewhere.[8k,l] A comparison of fluorescence quantum yields of fluoride adducts **3+F** and **4+F** with cyanide complexes **3+CN** and **4+CN** indicates that the cyanide adducts are better emitters than the fluoride adducts.

The association constants (for **3**: F^- binding 1.3×10^5 M^{-1}, CN^- binding 5.5×10^4 M^{-1}; for **4**, the total binding constant for F^- is 1.1 ± 10^{10} M^{-2}, while for CN^- it is 2.6 ± 10^9 M^{-2}) were calculated from their absorption spectral changes at 395 nm. These association constants are in good agreement with changes in absorption spectra upon addition of fluoride (pronounced decrease in absorption intensity) and cyanide (comparatively less decrease in absorption intensity) (Supporting Information). The detection limits of **3** and **4** toward fluoride ions were found to be 0.1 and 0.03 ppm, respectively, whereas for cyanide the detection limits were 1.41 and 0.71 ppm, respectively, for **3** and **4**. On the basis of these results, one can conclude that the response of

dx.doi.org/10.1021/ic402898n | Inorg. Chem. 2014, 53, 2776–2786

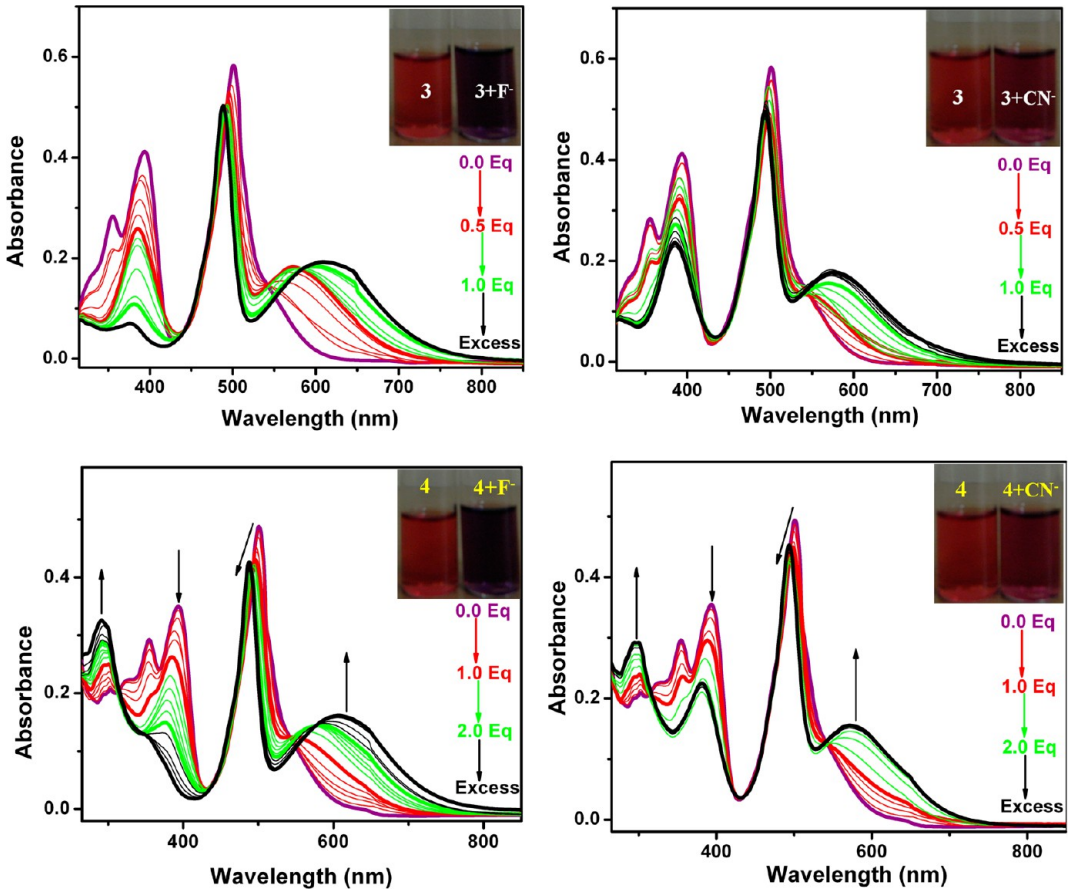

Figure 5. Absorption spectra of **3** (10.0 μM, $CHCl_3$) in the presence of TBAF (top left) and TBACN (top right) and **4** (10.0 μM, $CHCl_3$) in the presence of TBAF (bottom left) and TBACN (bottom right). (insets) The compounds **3** and **4** under ambient light before and after addition of F^- and CN^-.

compounds **3** and **4** is more pronounced for fluoride than it is for cyanide.

In presence of 100 equiv of fluoride/cyanide, compounds **3** and **4** show only the ^{11}B and ^{19}F signals corresponding to BODIPY ($-BF_2$) and $[(X-BAr_3)^-, X = F^- \text{ or } CN^-]$ (Supporting Information). This result excludes the possibility of BODIPY core decomposition in the presence of excess F^-/CN^-. Compounds **3** and **4** shows two ^{11}B signals at ~65 ppm (broad singlet) and ~1 ppm (sharp triplet), corresponding to tricoordinate (Ar_3B) and tetracoordinate (BODIPY) boron centers, respectively. Upon binding with F and CN, in the case of compound **3**, the signal corresponding to the Ar_3B unit disappeared, and a new peak appeared in the region of ~4 (Ar_3B-F) and ~10 ppm (Ar_3B-CN), respectively. Compound **4** also followed a similar trend (Ar_3B-F at 5 ppm and for Ar_3B-CN at 10 ppm). The ^{11}B NMR chemical shift for fluoroborates (Ar_3B-F) of **3** and **4** are upfield-shifted when compared to their respective cyanoborate complexes (Ar_3B-CN). The responses of **3** and **4** toward various other anions such as Cl^-, Br^-, I^-, ClO_4^-, NO_3^-, and CH_3COO^- were investigated (Figures 7 and 8). No changes in absorption and emission spectra of **3** and **4** were observed in titrations with these anions. Thus **3** and **4** act as selective chromogenic and fluorogenic sensors for F^- and CN^-.

Crystal Structure. The molecular and crystal structure of **4** is shown in Figure 9. Both the tricoordinate boron (B1 and B2) and tricoordinate N centers (TPA unit) adopt trigonal planar geometry. The metric parameters fall in the range of known triarylboron derivatives.[9b] The dihedral angles between the two boryl units and TPA unit differ significantly. The dihedral angle between 2CB2 (boryl) and the TPA is 11.7, and that between 2CB3 (boryl) and TPA is 31.6°. The dihedral angle between the phenyl moiety of the TPA unit and the indacene moiety is 53.7°. This higher dihedral angle value indicates that the electronic communication between the TPA and BODIPY units is weaker compared to the TPA and TAB interaction. In the solid state, the intermolecular C−H−F (C−H of the pyrrole moiety and F of the $-BF_2$ moiety) interaction between the neighboring molecules generates an interesting three-dimensional (3D) supramolecular structure.[10] The 3D structure contains discrete hydrophobic pockets, which are occupied by disordered solvent (hexane) molecules. Selected calculated bond lengths and angles are given in Table 3.

DFT Computational Studies. To rationalize the photophysical behavior of **3** and **4** and their respective fluoride bound complexes in a better way, density functional theory (DFT) computational studies were performed. For all calculations, the B3LYP hybrid functional and 6-31G(d) basis set were used as incorporated in the *Gaussian 09* software package.[11] Geometry optimizations were followed by consecutive frequency tests to ascertain stationary points. Figure 10 shows the B3LYP/6-31G(d) optimized structures of **3**, **4**, and their fluoride-bound entities $[\mathbf{3}+\mathbf{F}]^-$ and $[\mathbf{4}+\mathbf{2F}]^{2-}$.

As is evident from Figure 10, the electronically important molecular orbitals (MOs) are concentrated on different individual building units, and hence **3** and **4** retain most of the electronic signature of the building blocks. Despite having one

dx.doi.org/10.1021/ic402898n | *Inorg. Chem.* 2014, 53, 2776−2786

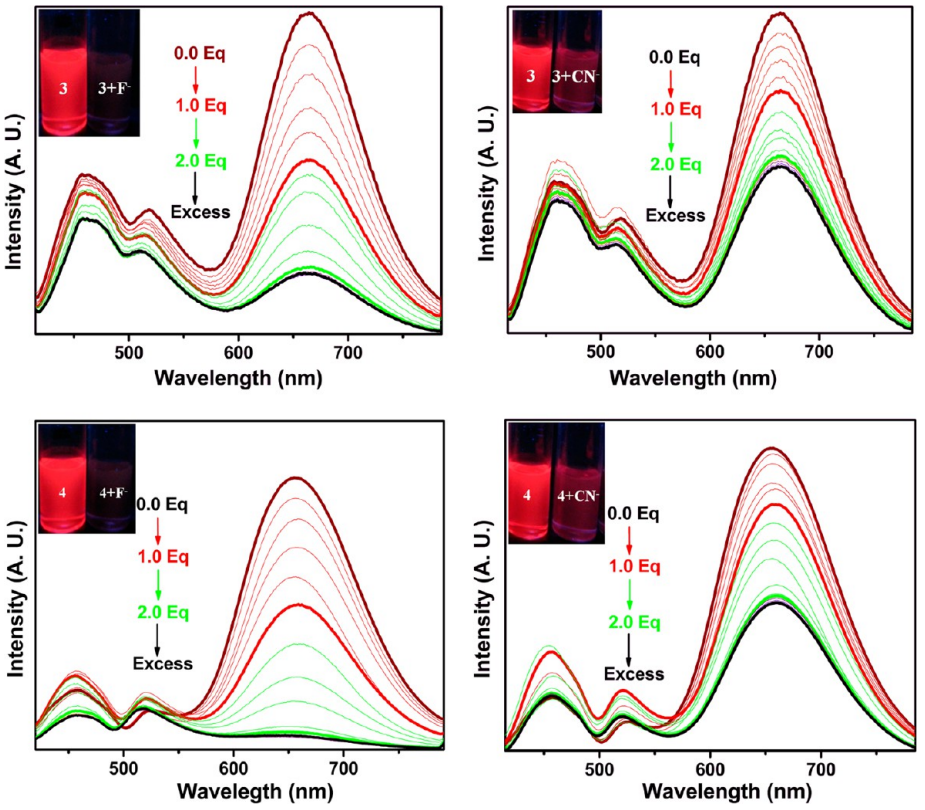

Figure 6. Fluorescence spectra of **3** (10.0 μM, $CHCl_3$; λ_{ex}= 400 nm) in the presence of TBAF (top left) and TBACN (top right). Fluorescence spectra of **4** (10.0 μM, $CHCl_3$; λ_{ex} = 400 nm) in the presence of TBAF (bottom left) and TBACN (bottom right). (insets) The compounds under UV light before and after addition of F^- and CN^-.

Table 2. Photophysical Data of Compounds 3 and 4[a]

compound	UV−vis (nm)/(ε/M^1 cm^{-1})	PL (nm)	Φ_f
3	300/1.75 × 10^4, 393/2.23 × 10^4, 500/5.84 × 10^4	457, 519, and 670	55
3+CN⁻	385/2.34 × 10^4, 493/5.84 × 10^4, 578/1.76 × 10^4	459[b], 515,[b] and 664[b]	41
3+F⁻	378/7.04 × 10^3, 487/5.04 × 10^4, 615/1.91 × 10^4	462[b], 513,[b] and 664[b]	15
4	325/1.71 × 10^4, 355/2.01 × 10^4, 385/ × 10^4, 500/5.84 × 10^4	450, 520, and 657	57
4+CN⁻	297/2.75 × 10^4, 381/2.03 × 10^4, 492/4.12 × 10^4, 573 × 10^4	459[b], 515,[b] and 657[b]	38
4+F⁻	292/3.28 × 104, 380/8.07 × 10^3, 487/5.84 × 10^4, 615/2.02 × 10^4	462[b], 513,[b] and 660[b]	16

[a]All given data are for 10 μM $CHCl_3$ solutions. [b]Fluorescence was quenching. [a]Fluorescence quantum yields were calculated using quinine sulfate solution (0.1 M, H_2SO_4, λ_{ex} = 400 nm, Φ_F = 57.7%) as reference and using the following formula: $\Phi = \Phi_F \times I \div I_R \times A_R \div A \times \eta^2 \div \eta_R^2$, where Φ = quantum yield, I = intensity of emission, A = absorbance at λ_{ex}, η = refractive index of solvent.

less triarylborane group, **3** showed high similarity with triad **4**, which was also evident from DFT studies. In **3** and **4**, the HOMO-1 and LUMO are concentrated on the BODIPY moiety and the HOMO orbitals are mainly localized on the TPA core, whereas the LUMO+1 is localized on the boryl unit. Clearly, the lowest-energy HOMO→LUMO transition represents the TPA→BODIPY charge transfer and HOMO→LUMO+1 represents high-energy TPA→boryl charge transfer phenomena. However, in the fluoride adducts, these ICT transitions are longer allowed, which clearly explains the quenching of higher-energy absorption bands upon fluoride addition to **3** and **4**. Noticeably, the HOMO→LUMO transitions in **3** and **4** represent triarylamine-to-BODIPY charge-transfer transition, which ultimately results in high Stokes' shifted BODIPY emission.

The fluoride adducts $[\mathbf{3+F}]^-$ and $[\mathbf{4 + 2F}]^{2-}$ have similar electronic structures. The HOMO-1 and HOMO orbitals are localized on the boryl moiety, whereas the LUMO is concentrated on the indacene unit. Thus the lowest-energy HOMO→LUMO and other transitions like the HOMO-1→LUMO transition represent fluoride-bound boryl-to-electron-accepting-BODIPY transition. Also, the HOMO−LUMO band gap was found to be much lower (Figure 10) than it was for free **3** and **4**. This clearly supports our assignment of the additional absorption band observed at ∼610 nm to borate-to-BODIPY ICT transition.

The electrostatic potential (ESP) surfaces of molecules **3** and **4** (Figure 11) also provided useful information to rationalize the photophysical properties. In **3** and **4**, the negative potentials around the mesityl moieties and the $-BF_2$-chelated BODIPY unit (which is a result of the high electronegativity of fluoride) induced a positive potential on the TPA unit. These results showcase the electron-withdrawing capabilities of the boryl and the BODIPY moieties. In the fluoride-bound complexes $[\mathbf{3+F}]^-$ and $[\mathbf{4 + 2F}]^{2-}$, the Ar_3BF unit has more negative potential, which partially affects the ESP over the BODIPY unit (see Figure 12). In the ground state, the negative charges are localized over the borane unit, which may be redistributed upon photo-excitation.

dx.doi.org/10.1021/ic402898n | Inorg. Chem. 2014, 53, 2776−2786

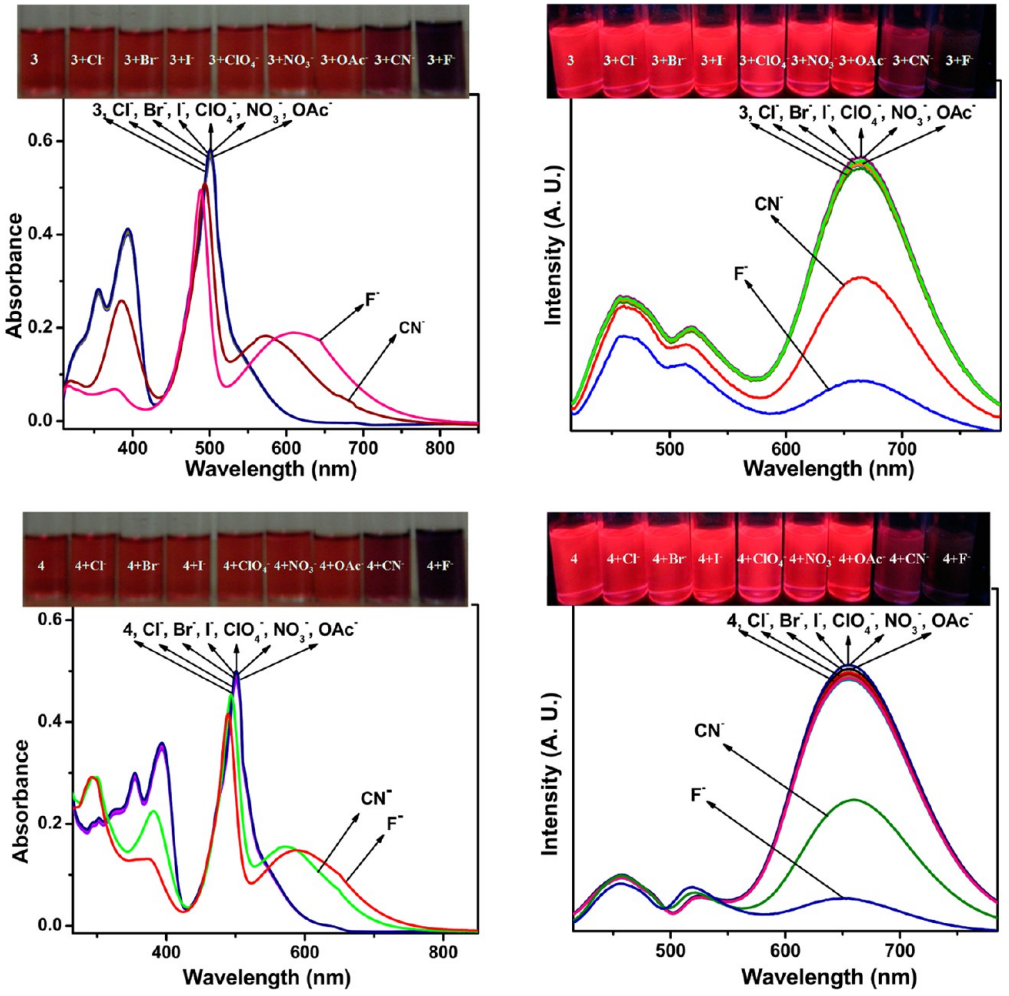

Figure 7. UV−vis (top left) and fluorescence spectra (top right) of **3** (10 μM in $CHCl_3$, λ_{ex} = 400 nm) in presence of different anions. (inset) Photograph of various anions under normal light (top left) and under UV light (top right). UV−vis (bottom left) and fluorescence spectra (bottom right) of **4** (10 μM in $CHCl_3$, λ_{ex} = 400 nm) in presence of different anions. (inset) Photograph of various anions under normal light (bottom left) and under UV light (bottom right).

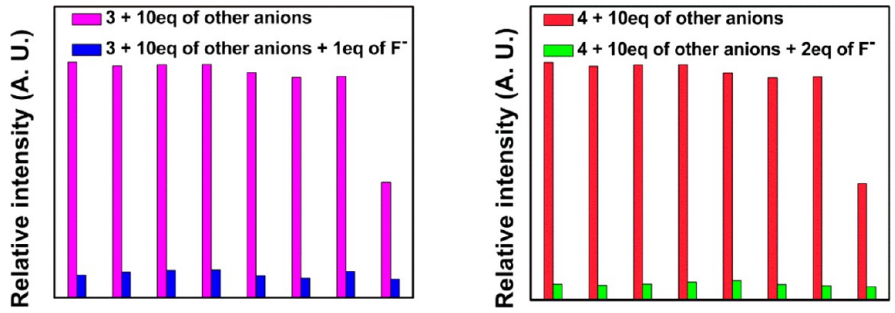

Figure 8. Competitive binding affinity of sensors **3** (left) and **4** (right) (10 μM in $CHCl_3$) toward F^- ions in the presence of 10.0 equiv of different anions (Cl^-, Br^-, I^-, ClO_4^-, NO_3^-, CH_3COO^-, and CN^- (left to right)).

CONCLUSIONS

A triad (**3**) and a tetrad (**4**) incorporating $-B(Mes)_2$, BODIPY, and TPA units were synthesized and characterized successfully. The attachment of two distinct electron-acceptor groups such as boryl and BODIPY into a single donor (TPA) unit induced two distinctive ICT processes in different energy regions of the absorption spectra. The two ICT processes are conveniently manipulated for detection of small anions. Compounds **3** and **4** efficiently act as chromogenic as well as fluorogenic sensors for F^- and CN^- ions (see Figure 13 for an example). The DFT-based computational investigations provide a reasonable understanding of events at molecular levels and correlate well with the experimental observations.

EXPERIMENTAL SECTION

n-Butyllithium (1.6 M in hexanes), triphenylamine, DDQ, and quinine sulfate were purchased from Aldrich, and pyrrole was purchased from SRL (India). All reactions were carried out under an atmosphere of purified nitrogen, using Schlenck techniques. THF and pyrrole were

dx.doi.org/10.1021/ic402898n | *Inorg. Chem.* 2014, 53, 2776−2786

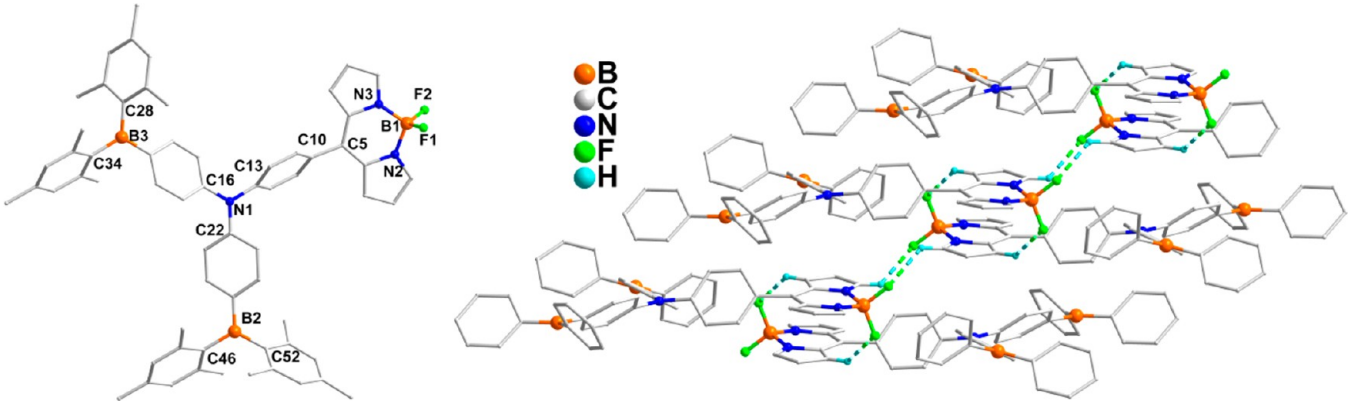

Figure 9. Molecular and supramolecular structure of **4**. C3−H3···F1 (2.875 Å and 130.2°) and C1−H1···F2 (2.335 Å and 131.2°).

Table 3. DFT-Obtained Selected Bond Lengths and Dihedral Angles

	3	**[3+F]$^-$**	**4**	**[4 + 2F]$^{2-}$**
bond lengths				
C−N (BMes-TPA)	1.418 Å	1.445 Å	1.421 Å, 1.421 Å	1.440 Å, 1.441 Å
C−N (PH-TPA)	1.429 Å	1.423 Å		
C−N (BDAr-TPA)	1.411 Å	1.392 Å	1.416 Å	1.377 Å
C−C (BODIPY-Ar)	1.476 Å	1.466 Å	1.478 Å	1.453 Å
dihedral angles				
C_3N−Mes_2BAr	39.44°	61.07°	40.48°, 40.98°	53.54°, 56.3°
C_3N−PH	48.91°	40.53°		
C_3N−(meso-aryl of BODIPY)	35.16°	22.65°	39.26°	17.99°

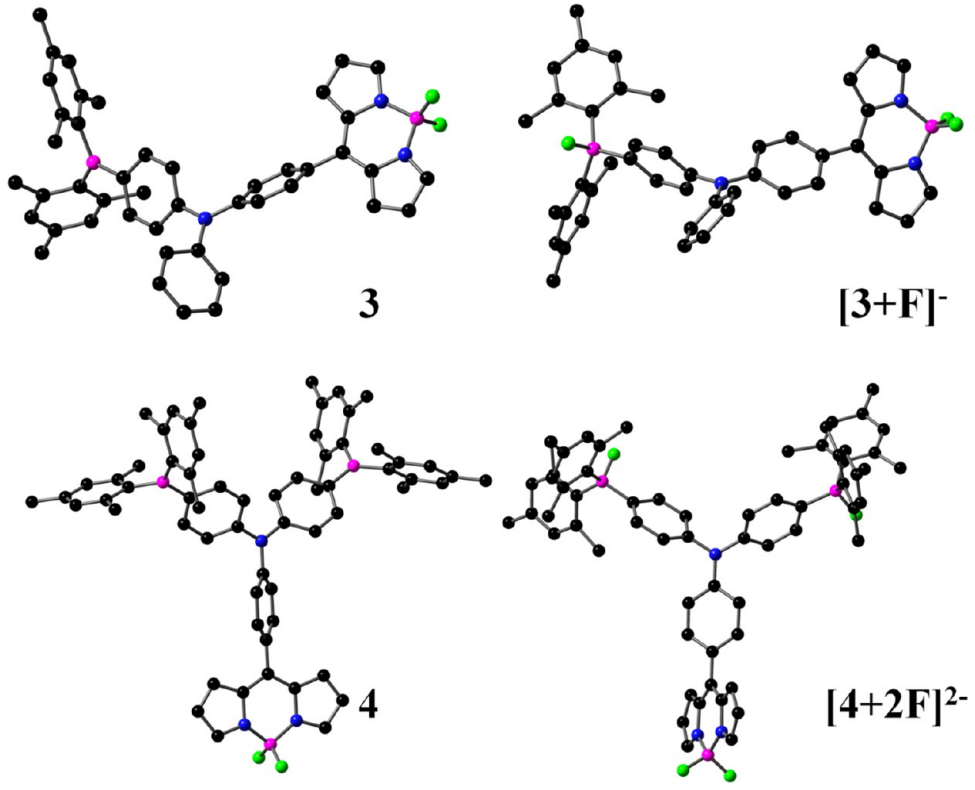

Figure 10. DFT B3LYP/6-31G(d) optimized geometries for **3**, [**3+F**]$^-$, **4**, and [**4+2F**]$^{2-}$ (Hydrogens are omitted for clarity. Color codes: C = black, N = blue, B = magenta, F = green).

distilled over sodium. Chlorinated solvents were distilled over CaH_2 and subsequently stored over 3 Å molecular sieves. The 400 MHz ^{1}H NMR, 376.5 MHz ^{19}F NMR, 100 MHz ^{13}C NMR, and 160.4 MHz ^{11}B NMR were recorded on a Bruker Advance 400 MHz NMR spectrometer. All solution ^{1}H and ^{13}C spectra were referenced internally to the solvent signal. ^{11}B and ^{19}F NMR spectra were referenced externally to $BF_3{\cdot}Et_2O$

dx.doi.org/10.1021/ic402898n | Inorg. Chem. 2014, 53, 2776−2786

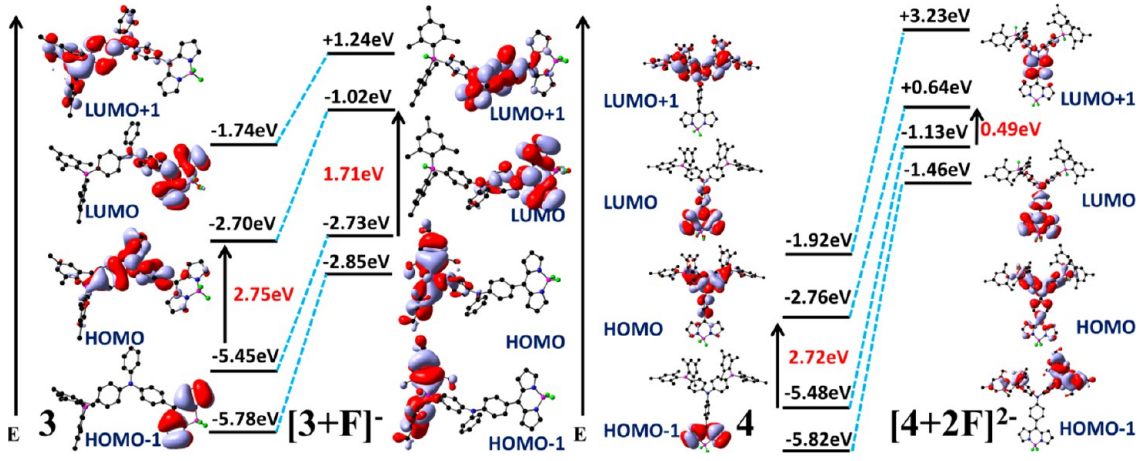

Figure 11. Selected MOs of **3**, $[3+F]^-$, **4**, and $[4 + 2F]^{2-}$ (not to scale; isovalue = 0.02).

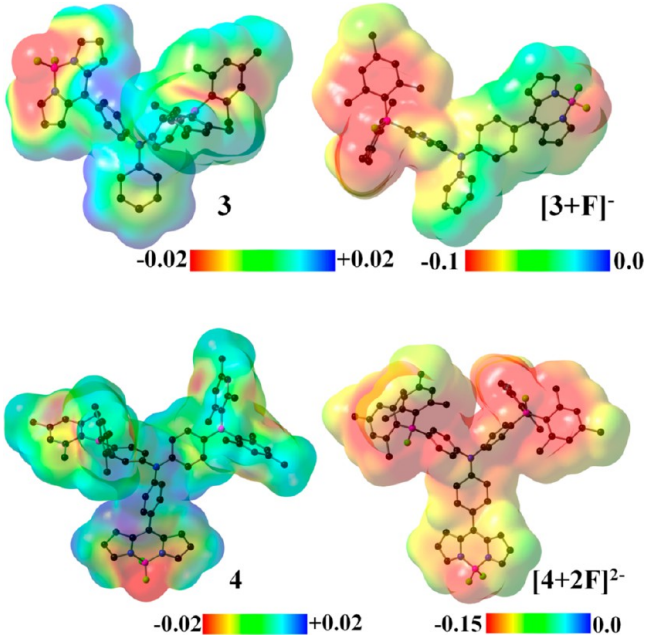

Figure 12. ESP surfaces of **3**, $[3+F]^-$, **4**, and $[4 + 2F]^{2-}$ (isovalue = 0.0004).

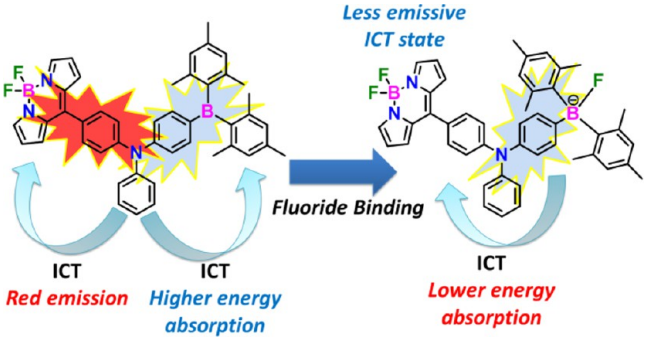

Figure 13. Important electronic events in free triad **3** and $[3+F]^-$.

(δ = 0) in C_6D_6. High-resolution mass spectra were obtained from Q-TOF instrument by electrospray ionization (ESI). Electronic absorption spectra were recorded on a Perkin-Elmer LAMBDA 750 ultraviolet–visible (UV-vis) spectrophotometer. Compounds were weighed using a microbalance (±0.1 mg), and solutions were made in volumetric glassware and then charged in quartz cuvettes with sealing screw caps. Fluorescence emission studies were carried out on a Horiba JOBIN YVON Fluoromax-4 spectrometer. Compounds **3** (1×10^{-5} M) and **4** (1×10^{-5} M) were dissolved in degassed $CHCl_3$ and 3 mL of solution charged in quartz cuvettes with sealing screw caps. Compounds **3** and **4** were titrated with incremental addition of TBAF (1.5×10^{-3} M) and TBACN (1.5×10^{-3} M) diluted in $CHCl_3$ solution. Single-crystal X-ray diffraction studies were carried out with a Bruker SMART APEX diffractometer equipped with a three-axis goniometer. The crystals were kept under a steady flow of cold N_2 during the data collection. The data were integrated using SAINT,[12a] and an empirical absorption correction was applied with SADABS. The structures were solved by direct methods and refined by full-matrix least-squares on F^2 using SHELXTL software.[12b] All the non-hydrogen atoms were refined with anisotropic displacement parameters, while the hydrogen atoms were refined isotopically on the positions calculated using a riding model.

Synthesis of 1a (4-bromo-*N*-(4-(diethoxymethyl)phenyl)-*N*-phenylaniline). Triethylorthoformate (7.2 g,48.43 mmol) and 4-((4-bromophenyl)(phenyl)amino)benzaldehyde (5.0 g, 14.24 mmol) were dissolved in ethanol, and then a catalytic amount of concentrated HCl was added to the solution. The resultant solution was refluxed for 4 h. When thin-layer chromatography showed the complete consumption of aldehyde, the reaction mixture was brought to room temperature and extracted with a mixture of cold water and ethyl acetate. The combined organic layer was washed with brine and dried over anhydrous Na_2SO_4. The volatiles removed under reduced pressure afforded **1a** as colorless liquid. Yield: 14.28 g, 99%. ^{1}H NMR (400 MHz, $CDCl_3$ δ ppm) δ 7.35 (m, 4H), 7.30 (m, 2H), 7.05 (m, 5H), 6.95 (m, 2H) 5.45 (s, 1H), 3.67 (m, 4H), 1.27 (t, J = 6.8 Hz, 7.2 Hz 6H). ^{13}C NMR (100.00 MHz, $CDCl_3$, δ ppm) 147.8, 147.3, 134.2, 132.8, 129.8, 128.1, 126.1, 125.8, 125.0, 124.8, 123.8, 115.4, 101.9, 61.7, 15.7.

Synthesis of 1b (4-bromo-*N*-(4-bromophenyl)-*N*-(4-(diethoxymethyl)phenyl)aniline). Compound **1b** was prepared following a procedure similar to that used for compound **1a**. The quantities involved and characterization data are as follows. Triethylorthoformate (3.5 g, 23.78 mmol), 4-(bis(4-bromophenyl)-amino)benzaldehyde (3.0 g, 6.99 mmol), and HCl (one drop). ^{1}H NMR (400 MHz, $CDCl_3$ δ ppm) 7.36 (m, 6H), 7.03 (d, J = 8 Hz 2H), 6.94 (m, 4H), 5.44 (s, 2H), 3.67 (m, 8H), 1.27 (t, J = 6.8 Hz, 7.2 Hz 6H). ^{13}C NMR (100.00 MHz, $CDCl_3$, δ ppm) 152.8, 148.5, 133.4, 131.9, 130.5, 127.9, 120.9, 118.6, 109.5, 65.7, 16.5.

Synthesis of 2a (4-((4-(dimesitylboryl)phenyl)(phenyl)-amino)benzaldehyde). Compound **1a** (2.0 g, 4.70 mmol) was dissolved in dry THF and degassed by purging with N_2 for 30 min followed by cooling to −78 °C (acetone/liquid N_2). *n*-Butyllithium (3.5 mL, 5.64 mmol, 1.6 M solution in hexane) was added over 30 min. After 1 h, a solution of dimesitylfluoroborane (1.5 g, 5.64 mmol) in 15 mL of dry THF was added over 10 min. The reaction mixture was allowed to warm to room temperature, and stirring was continued for 12 h. After 12 h, 30 mL of 1N HCl was added, and stirring was continued for another 4 h; then the reaction mixture was extracted with ether. The combined

dx.doi.org/10.1021/ic402898n | Inorg. Chem. 2014, 53, 2776–2786

organic layers were washed with brine solution and dried over anhydrous Na_2SO_4. Evaporation of the solvents under reduced pressure yielded crude product. Crude product was purified by alumina column chromatography, using a mixture of petroleum ether and ethyl acetate (8:2). Yield: 1.82 g, 74%. ^{1}H NMR (399.99 MHz, $CDCl_3$ δ ppm) 9.86 (s, 1H), 7.75 (d, J = 8 Hz, 2H), 7.72 (d, J = 8.4 Hz, 2H), 1.10 (m, 1H), 7.17 (m, 4H), 7.06 (m, 4H), 6.83 (s, 4H), 2.31 (s, 6H), 2.08 (s, 12H). ^{13}C NMR (100.00 MHz, $CDCl_3$, δ ppm) 151.7, 148.2, 147.2, 145.7, 144.2, 142.1, 141.3, 138.7, 137.5, 136.1, 134.5, 131.1, 130.4, 128.9, 127.2, 126.0, 125.1, 121.7, 118.7, 23.7, 21.3.

Synthesis of 2b (4-(dimesitylboryl)-*N*-(4-(dimesitylboryl)-phenyl)-*N*-phenylaniline). Compound **2a** was prepared following a procedure similar to that used for compound **1b**. The quantities involved and characterization data are as follows. Compound **1b** (2.0 g, 3.97 mmol), *n*-butyllithium (2.9 mL, 4.77 mmol, 1.6 M solution in hexane), dimesitylfluoroborane (1.3 g, 5.64 mmol). Yield: 1.75 g, 57%. ^{1}H NMR (399.99 MHz, $CDCl_3$ δ ppm) 9.88 (s, 1H), 7.78 (d, J = 8.4 Hz, 2H), 7.48 (d, J = 8.4 Hz, 4H), 7.23 (d, J = 8.4 Hz, 2H), 7.09 (d, J = 8.4 Hz, 4H), 6.83 (s, 8H), 2.31 (s, 12H), 2.06 (s, 24H). ^{13}C NMR (100.0 MHz, $CDCl_3$, δ ppm) 191.0, 152.5, 149.7, 141.3, 139.0, 131.7, 128.6, 127.3, 124.5, 123.3, 23.9, 21.6.

Synthesis of New Triad 3. Pyrrole (2.7 mL, 38.35 mmol) and **2a** (0.5 g, 0.96 mmol) were stirred at room temperature under nitrogen atmosphere for 30 min, and $BF_3{\cdot}Et_2O$ (one drop) was added. After complete consumption of **2a**, DDQ (0.1 g, 0.47 mmol) was added, and stirring was continued for another 6 h. The resultant solution was allowed to react with triethylamine (0.45 mL, 3.13 mmol) followed by $BF_3{\cdot}Et_2O$ (0.4 mL, 3.13 mmol). After stirring for 5 h at RT, solvents were removed under vacuum to give crude product. It was further purified by silica gel column chromatography (1:9 ethylacetate/petroleum ether) to give compound **3** as a red solid. Yield: 0.18 g, 60%. ^{1}H NMR (399.99 MHz, $CDCl_3$ δ ppm) 7.92 (s, 2H), 7.48 (m, 4H), 7.28 (d, J = 8.4 Hz, 2H), 7.25 (m, 5H), 7.09 (m, 4H), 6.82 (s, 4H), 6.57 (d, J = 2.0 Hz, 2H), 2.30 (s, 6H), 2.07 (s, 12H). ^{13}C NMR (100.0 MHz, $CDCl_3$, δ ppm) 150.5, 147.6, 146.5, 143.6, 142.1, 141.1, 140.8, 138.8, 135.1, 132.6, 131.6, 130.3, 128.5, 127.2, 125.8, 122.6, 118.6, 23.9, 21.6. ^{11}B NMR (160 MHz, $CDCl_3$, δ ppm) 0.23 (t, J = 36 Hz) and 61, ^{19}F NMR (376 MHz, $CDCl_3$, δ ppm) −145.06 (q). MS (TOF-ESI) (m/z): calcd for 932.52 $[M]^+$; found, 932.52 $[M]^+$. Calcd for 912.62 $[M - F]^+$; found, 912.75 $[M - F]^+$.

Synthesis of New Tetrad 4. Compound **4** was prepared following a procedure similar to that used for compound **3**. The quantities involved and characterization data are as follows. Compound **2b** (0.5 g, 0.65 mmol), pyrrole (1.8 mL, 26.02 mmol), DDQ (0.76 g, 0.34 mmol), triethylamine (0.3 mL, 2.22 mmol), $BF_3{\cdot}OEt_2$ (0.25 mL, 2.22 mmol). Yield: 0.12 g, 57%. ^{1}H NMR (399.99 MHz, $CDCl_3$ δ ppm) 7.91 (s, 2H), 7.52 (m, 4H), 7.49 (d, J = 8.4 Hz 2H), 7.28 (d, J = 8.4 Hz, 2H), 7.12 (d, J = 8.4 Hz, 2H), 7.04 (d, J = 4.4 Hz, 2H), 6.83 (s, 8H), 6.57 (d, J = 2 Hz, 2H), 2.31 (s, 12H), 2.06 (s, 24H). ^{1}H NMR (399.99 MHz, $CDCl_3$ δ ppm) 149.9, 147.4, 143.8, 142.1, 141.2, 138.9, 135.1, 132.6, 129.1, 128.6, 124.1, 123.9, 118.7, 23.9, 21.6. ^{11}B NMR (160 MHz, $CDCl_3$, δ ppm) 0.27 (t, J = 36 Hz) and 65, ^{19}F NMR (376 MHz, $CDCl_3$, δ ppm) −146.21 (q). MS (TOF-ESI) (m/z): calcd for 683.4459 $[M]^+$; found, 683.4974 $[M]^+$. Calcd for 664.3471 $[M - F]^+$; found, 664.8891 $[M - F]^+$.

■ ASSOCIATED CONTENT

Ⓢ Supporting Information

UV−vis and PL spectra, X-ray crystallographic refinement data, fluorescence decay profile, ^{1}H, ^{13}C, and ^{19}F NMR spectra, DFT computational data and CIF file. This material is available free of charge via the Internet at http://pubs.acs.org.

■ AUTHOR INFORMATION

Corresponding Author

*E-mail: thilagar@ipc.iisc.ernet.in. Fax: 0091-80-23601552. Phone: 0091-80-22933353.

Notes

The authors declare no competing financial interest.

■ ACKNOWLEDGMENTS

P.T. thanks the Department of Science and Technology (DST) of New Delhi and the ISRO-IISc Space Technology Cell for the financial support. We acknowledge the Supercomputer Education and Research Centre, Indian Institute of Science, for computing facilities. Mr. A.S. thanks the Indian Institute of Science (IISc), Bangalore, for research fellowship.

■ REFERENCES

(1) (a) Ward, M. D. *Chem. Soc. Rev.* **1995**, *24*, 121. (b) Ward, M. D. *Chem. Soc. Rev.* **1997**, *26*, 365. (c) Choppinet, P.; Jullien, L.; Valeur, B. *J. Chem. Soc., Perkin Trans.* **1999**, *2*, 249. (d) Serin, J. M.; Brousmiche, D. W.; Frechet, J. M. J. *Chem. Commun.* **2002**, 2605. (e) Weil, T.; Reuther, E.; Mullen, K. *Angew. Chem., Int. Ed.* **2002**, *41*, 1900. (f) Metivier, R.; Kulzer, F.; Weil, T.; Mullen, K.; Basche, T. *J. Am. Chem. Soc.* **2004**, *126*, 14365. (g) De Schryver, F. C.; Vosch, T.; Cotlet, M.; Auweraer, M. V. R.; Mullen, K.; Hofkens, J. *Acc. Chem. Res.* **2005**, *38*, 514. (h) Cotlet, M.; Vosch, T.; Habichi, S.; Weil, T.; Mullen, K.; Hofkens, J.; De Schryver, F. *J. Am. Chem. Soc.* **2005**, *127*, 9760. (i) Valeur, B.; Leray, I. *Inorg. Chim. Acta* **2007**, *360*, 765. (j) Balzani, V.; Credi, A.; Venturi, M. *Molecular Devices and Machines—Concepts and Pespectives for the Nanoworld,* 2nd ed.; Wiley-VCH: Weinheim, Germany, 2008. (k) Nastasi, F.; Puntoriero, F.; Campagna, S.; Diring, S.; Ziessel, R. *Phys. Chem. Chem. Phys.* **2008**, *10*, 3982. (l) Balzani, V.; Bergamini, G.; Ceroni, P. *Coord. Chem. Rev.* **2008**, *252*, 2456. (m) Diring, S.; Puntoriero, F.; Nastasi, F.; Campagna, S.; Ziessel, R. *J. Am. Chem. Soc.* **2009**, *131*, 6108. (n) Harriman, A.; Mallon, L. J.; Elliot, K. J.; Haefele, A.; Ulrich, G.; Ziessel, R. *J. Am. Chem. Soc.* **2009**, *131*, 13375. (o) Weil, T.; Vosch, T.; Hofkens, J.; Peneva, K.; Mullen, K. *Angew. Chem., Int. Ed.* **2010**, *49*, 9068. (p) Gust, D.; Andreasson, J.; Pischel, U.; Moore, T. A.; Moore, A. L. *Chem. Commun.* **2012**, *48*, 1947. (q) Kostereli, Z.; Ozdemir, T.; Buyukcakir, O.; Akkaya, E. U. *Org. Lett.* **2012**, *14*, 3636. (r) Diring, S.; Ventura, B.; Barbieri, A.; Ziessel, R. *Dalton Trans.* **2012**, *41*, 13090.

(2) (a) Yilmaz, M. D.; Bozdemir, O. A.; Akkaya, E. U. *Org. Lett.* **2006**, *8*, 2871. (b) Flamigni, L.; Collin, J.-P.; Sauvage, J.-P. *Acc. Chem. Res.* **2008**, *41*, 857. (c) Lee, C. Y.; Jang, J. K.; Kim, C. H.; Jung, J.; Park, B. K.; Park, J.; Choi, W.; Han, Y.-K.; Joo, T.; Park, J. T. *Chem.—Eur. J.* **2010**, *16*, 5586. (d) Schwartz, E.; Gac, S. L.; Cornelissen, J. J. L. M.; Nolte, R. J. M.; Rowan, A. E. *Chem. Soc. Rev.* **2010**, *39*, 1576. (e) Warnan, J.; Buchet, F.; Pellegrin, Y.; Blart, E.; Odobel, F. *Org. Lett.* **2011**, *13*, 3944. (f) Ziessel, R.; Harriman, A. *Chem. Commun.* **2011**, *47*, 611. (g) Bonaccorsi, P.; Aversa, M. C.; Barattucci, A.; Papalia, T.; Puntoriero, F.; Campagna, S. *Chem. Commun.* **2012**, *48*, 10550. (h) Brizet, B.; Eggenspiller, A.; Gros, C. P.; Barbe, J.-M.; Goze, C.; Denat, F.; Harvey, P. D. *J. Org. Chem.* **2012**, *77*, 3646. (i) Warnan, J.; Pellegrin, Y.; Blart, E.; Odobel, F. *Chem. Commun.* **2012**, *48*, 675. (j) Lazarides, T.; Kuhri, S.; Charalambidis, G.; Panda, M. K.; Guldi, D. M.; Coutsolelos, A. G. *Inorg. Chem.* **2012**, *51*, 4193. (k) Barbieri, A.; Ventura, B.; Ziessel, R. *Coord. Chem. Rev.* **2012**, *256*, 1732. (l) Yang, J.; Yoon, M.-C.; Yoo, H.; Kim, P.; Kim, D. *Chem. Soc. Rev.* **2012**, *41*, 4808. (m) Odobel, F.; Pellegrin, Y.; Warnan, J. *Energy Environ. Sci.* **2013**, *6*, 204.

(3) (a) Schroeyers, W.; Vallee, R.; Patra, D.; Hofkens, J.; Habuchi, S.; Vosch, T.; Cotlet, M.; Mullen, K.; Enderlein, J.; Schryver, F. C. De *J. Am. Chem. Soc.* **2004**, *126*, 14310. (b) Bhalla, V.; Roopa; Kumar, M.; Sharma, P. R.; Kaur, T. *Inorg. Chem.* **2012**, *51*, 2150. (c) Li, Y.; Cao, L.; Tian, H. *J. Org. Chem.* **2006**, *71*, 8279. (d) Montes, V. A.; Bolivar, C. P.; Agarwal, N.; Shinar, J.; Anzenbacher, P., Jr. *J. Am. Chem. Soc.* **2006**, *128*, 12436. (e) Oesterling, I.; Mullen, K. *J. Am. Chem. Soc.* **2007**, *129*, 4595. (f) Lee, M. H.; Quang, D. T.; Jung, H. S.; Yoon, J.; Lee, C.-H.; Kim, J. S. *J. Org. Chem.* **2007**, *72*, 4242. (g) Kanibolotsky, A. L.; Perepichka, I. F.; Skabara, P. J. *Chem. Soc. Rev.* **2010**, *39*, 2695. (h) Nierth, A.; Kobitski, A. Y.; Nienhaus, G. U.; Jaschke, A. *J. Am. Chem. Soc.* **2010**, *132*, 2646. (i) Sarma, M.; Chatterjee, T.; Ghanta, S.; Das, S. K. *J. Org. Chem.* **2012**, *77*, 432. (j) Lee, C.-C.; Leung, M.-k.; Lee, P.-Y.; Chiu, T.-L.; Lee, J.-H.; Liu, C.; Chou, P.-T. *Macromolecules* **2012**, *45*, 751.

(4) (a) Loudet, A.; Burgess, K. *Chem. Rev.* **2007**, *107*, 4891. (b) Wood, T. E.; Thompson, A. *Chem. Rev.* **2007**, *107*, 1831. (c) Ziessel, R.; Ulrich, G.; Harriman, A. *New J. Chem.* **2007**, *31*, 496. (d) Ulrich, G.; Ziessel, R.; Harriman, A. *Angew. Chem., Int. Ed.* **2008**, *47*, 1184. (e) Benniston, A. C. *Phys. Chem. Chem. Phys.* **2009**, *11*, 4124. (f) Neponnyashchii, A. B.; Bard, A. J. *Acc. Chem. Res.* **2012**, *45*, 1844. (g) Boens, N.; Leen, V.; Dehaen, W. *Chem. Soc. Rev.* **2012**, *41*, 1130. (h) Awuah, S. G.; You, Y. *RSC Adv.* **2012**, *2*, 11169. (i) Kamkaew, A.; Lim, S. H.; Lee, H. B.; Kiew, L. V.; Chung, L. Y.; Burgess, K. *Chem. Soc. Rev.* **2013**, *42*, 77. (j) Zhao, J.; Wu, W.; Sun, J.; Guo, S. *Chem. Soc. Rev.* **2013**, *42*, 5323. (k) Carlson, J. C. T.; Meimetis, L. G.; Hilderbrand, S. A.; Weissleder, R. *Angew. Chem., Int. Ed.* **2013**, *52*, 6917. (l) Khan, T. K.; Broring, M.; Mathur, S.; Ravikanth, M. *Coord. Chem. Rev.* **2013**, *257*, 2348. (m) Madhu, S.; Gonnade, R.; Ravikanth, M. *J. Org. Chem.* **2013**, *78*, 5056.

(5) (a) Shirota, Y.; Kinoshita, M.; Noda, T.; Okumoto, K.; Ohara, T. *J. Am. Chem. Soc.* **2000**, *122*, 11021. (b) Entwistle, C. D.; Marder, T. B. *Angew. Chem., Int. Ed.* **2002**, *41*, 2927. (c) Doi, H.; Kinoshita, M.; Okumoto, K.; Shirota, Y. *Chem. Mater.* **2003**, *15*, 1080. (d) Entwistle, C. D.; Marder, T. B. *Chem. Mater.* **2004**, *16*, 4574. (e) Yamaguchi, S.; Wakamiya, A. *Pure Appl. Chem.* **2006**, *78*, 1413. (f) Heilmann, J. B.; Scheibitz, M.; Qin, Y.; Sundararaman, A.; Jakle, F.; Kretz, T.; Bolte, M.; Lerner, H. W.; Holthausen, M. C.; Wagner, M. *Angew. Chem., Int. Ed.* **2006**, *45*, 920. (g) Hudnall, T. W.; Chiu, C.-W.; Gabbai, F. P. *Acc. Chem. Res.* **2009**, *42*, 388−397. (h) Hudson, Z. M.; Wang, S. *Acc. Chem. Res.* **2009**, *42*, 1584. (i) Jakle, F. *Chem. Rev.* **2010**, *110*, 3985. (j) Wade, C. R.; Broomsgrove, A. E. J.; Aldridge, S.; Gabba1, F. P. *Chem. Rev.* **2010**, *110*, 3958. (k) Bresner, C.; Haynes, C. J. E.; Addy, D. A.; Broomsgrove, A. E. J.; Fitzpatrick, P.; Vidovic, D.; Thompson, A. L.; Fallis, I. A.; Aldridge, S. *New J. Chem.* **2010**, *34*, 1652. (l) Cataldo, S.; Fabiano, S.; Ferrante, F.; Previti, F.; Patane, S.; Pignataro, B. *Macromol. Rapid Commun.* **2010**, *31*, 1281. (m) Feng, J.; Tian, K.; Hu, D.; Wang, S.; Li, S.; Zeng, Y.; Li, Y.; Yang, G. *Angew. Chem., Int. Ed.* **2011**, *50*, 8072. (n) Chen, P.; Jakle, F. *J. Am. Chem. Soc.* **2011**, *133*, 20142. (o) Tanaka, K.; Chujo, Y. *Macromol. Rapid Commun.* **2012**, *33*, 1235. (p) Vadavi, R. S.; Kim, H.; Lee, K. M.; Kim, T.; Lee, J.; Lee, Y. S.; Lee, M. H. *Organometallics* **2012**, *31*, 31. (q) Zhao, H.; Reibenspies, J. H.; Gabba1, F. P. *Dalton Trans.* **2013**, *42*, 608. (r) Saito, S.; Matsuo, K.; Yamaguchi, K. *J. Am. Chem. Soc.* **2012**, *134*, 9130. (s) Chen, P.; Lalancette, R. A.; Jakle, F. *Angew. Chem., Int. Ed.* **2012**, *51*, 7994. (t) Varlan, M.; Blight, B. A.; Wang, S. *Chem. Commun.* **2012**, *48*, 12059. (u) Blight, B. A.; Guillet-Nicolas, R.; Kleitz, F.; Wang, R.-Y.; Wang, S. *Inorg. Chem.* **2013**, *52*, 1673. (v) Hoffend, C.; Diefenbach, M.; Januszewski, E.; Bolte, M.; Lerner, H.-W.; Holthausen, M. C.; Wagner, M. *Dalton Trans.* **2013**, *42*, 13826.

(6) (a) Huh, J. O.; Do, Y.; Lee, M. H. *Organometallics* **2008**, *27*, 1022. (b) Fu, G.-L.; Pan, H.; Zhao, Y.-H.; Zhao, C.-H. *Org. Biomol. Chem.* **2011**, *9*, 8141. (c) Sun, H.; Dong, X.; Liu, S.; Zhao, Q.; Mou, X.; Yang, H. Y.; Huang, W. *J. Phys. Chem. C* **2011**, *115*, 19947. (d) Yin, Z.; Tam, A. Y.; Wong, K. M.; Tao, C.; Li, B.; Poon, C.; Wu, L.; Yam, V. W. *Dalton Trans.* **2012**, *41*, 11340. (e) Lu, J.-s.; Ko, S.-B.; Walters, N. R.; Wang, S. *Org. Lett.* **2012**, *14*, 5660. (f) Swamy, P. C. A.; Mukherjee, S.; Thilagar, P. *Chem. Commun.* **2013**, *49*, 993.

(7) (a) Pron, A.; Baumgarten, M.; Mu llen, K. *Org. Lett.* **2010**, *12*, 4236. (b) Schmidt, H. C.; Reuter, L. G.; Hamacek, J.; Wenger, O. S. *J. Org. Chem.* **2011**, *76*, 9081. (c) Pan, H.; Fu, G.-L.; Zhao, Y.-H.; Zhao, C.-H. *Org. Lett.* **2011**, *13*, 4830. (d) Makarov, N. S.; Mukhopadhyay, S.; Yesudas, K.; Brédas, J.-L.; Perry, J. W.; Pron, A.; Kivala, M.; Müllen, K. *J. Phys. Chem. A* **2012**, *116*, 3781. (e) Ito, A.; Kang, Y.; Saito, S.; Sakuda, E.; Kitamura, N. *Inorg. Chem.* **2012**, *51*, 7722. (f) Fu, G.-L.; Zhang, H.-Y.; Yan, Y.-Q.; Zhao, C.-H. *J. Org. Chem.* **2012**, *77*, 1983. (g) Sudhakar, P.; Mukherjee, S.; Thilagar, P. *Organometallics* **2013**, *32*, 3129.

(8) (a) Lager, E.; Liu, J.; Aguilar-Aguilar, A.; Tang, B. Z.; Pena-Cabrera, E. *J. Org. Chem.* **2009**, *74*, 2053. (b) Hu, R.; Lager, E.; Aguilar-Aguilar, A.; Liu, J.; Lann, J. W. Y.; Sung, H. H. Y.; Williams, I. D.; Zhong, Y.; Wong, K. S.; Pena-Cabrera, E.; Tang, B. Z. *J. Phys. Chem. C* **2009**, *113*, 15845. (c) Sakuda, E.; Ando, Y.; Ito, A.; Kitamura, N. *J. Phys. Chem. A* **2010**, *114*, 9144. (d) Mataga, N.; Kubota, T. *Molecular Interactions and Electronic Spectra;* Marcel Dekker: New York, 1970. (e) Collado, D.; Casado, J.; Gonzalez, S. R.; Navarrete, J. T. L.; Suau, R.; Perez-Inestrosa, E.; Pappenfus, T. M.; Raposo, M. M. M. *Chem.—Eur. J.* **2011**, *17*, 498. (f) Chen, Y.; Zhao, J.; Guo, H.; Xie, L. *J. Org. Chem.* **2012**, *77*, 2192. (g) Mao, M.; Ren, M. G; Song, Q. H. *Chem.—Eur. J.* **2012**, *18*, 15512. (h) Ren, M. G; Mao, M.; Song, Q. H. *Chem. Commun.* **2012**, *48*, 2970. (i) Yuan, M. S; Liu, Z. Q; Fang, Q. *J. Org. Chem.* **2007**, *72*, 7915. (j) Hu, R.; Lager, E.; Aguilar-Aguilar, A.; Liu, J.; Lann, J. W. Y.; Sung, H. H. Y.; Williams, I. D.; Zhong, Y.; Wong, K. S.; Pena-Cabrera, E.; Tang, B. Z. J. *Phys. Chem. C* **2009**, *113*, 15845. (k) Wade, C. R.; Gabbai, F. P. *Inorg. Chem.* **2010**, *49*, 714. (l) Miyasaka, S.; Kobayashi, J.; Kawashima, T. *Tetrahedron Lett.* **2009**, *50*, 3467. (m) Mayer, U.; Gutmann, V.; Gerger, W. *Monatsh. Chem.* **1975**, *106*, 1235.

(9) (a) Lakowicz, J. R. *Principles of Fluorescence Spectroscopy,* 3rd ed.; Kluwer Academics/Plenum Publisher: New York, 2006. (b) Zhao, H.; Gabbaï, F. P. *Organometallics* **2012**, *31*, 2327. (c) Banuelos, J.; Arroyo-Cordoba, I. J.; Valois-Escamilla, I.; Alvarez-Hernandez, A.; Pena-Cabrera, E.; Hu, R.; Tang, B. Z.; Esnal, I.; Martıneza, V.; Arbeloa, I. L. *RSC Adv.* **2011**, *1*, 677. (d) Leriche, P.; Frere, P.; Cravino, A.; Aleveque, O.; Roncali, J. *J. Org. Chem.* **2007**, *72*, 8332.

(10) (a) Dhokale, B.; Gautam, P.; Mobin, S. M.; Misra, R. *Dalton Trans.* **2013**, *42*, 1512. (b) Swamy, P. C. A.; Mukherjee, S.; Thilagar, P. *J. Mater. Chem. C* **2013**, *1*, 4691.

(11) Frisch, M. J.; Trucks, G. W.; Schlegel, H. B.; Scuseria, G. E.; Robb, M. A.; Cheeseman, J. R.; Scalmani, G.; Barone, V.; Mennucci, B.; Petersson, G. A.; Nakatsuji, H.; Caricato, M.; Li, X.; Hratchian, H. P.; Izmaylov, A. F.; Bloino, J.; Zheng, G.; Sonnenberg, J. L.; Hada, M.; Ehara, M.; Toyota, K.; Fukuda, R.; Hasegawa, J.; Ishida, M.; Nakajima, T.; Honda, Y.; Kitao, O.; Nakai, H.; Vreven, T.;Montgomery, J. A., Jr.; Peralta, J. E.; Ogliaro, F.; Bearpark, M.; Heyd, J. J.; Brothers, E.; Kudin, K. N.; Staroverov, V. N.; Kobayashi, R.; Normand, J.; Raghavachari, K.; Rendell, A.; Burant, J. C.; Iyengar, S. S.; Tomasi, J.; Cossi,M.; Rega,N.; Millam, N. J.; Klene,M.; Knox, J. E.; Cross, J. B.; Bakken, V.; Adamo, C.; Jaramillo, J.; Gomperts, R.; Stratmann, R. E.; Yazyev, O.; Austin, A. J.; Cammi, R.; Pomelli, C.; Ochterski, J. W.; Martin, R. L.; Morokuma, K.; Zakrzewski, V. G.; Voth, G. A.; Salvador, P.; Dannenberg, J. J.; Dapprich, S.; Daniels, A. D.; Farkas, O .; Foresman, J. B.; Ortiz, J. V.; Cioslowski, J.; Fox, D. J. *Gaussian 09,* Revision C.01; Gaussian, Inc.: Wallingford, CT, 2010.

(12) (a) *SAINT-NT,* Version 6.04; Bruker AXS: Madison, WI, 2001. (b) *SHELXTL-NT,* Version 6.10; Bruker AXS: Madison, WI, 2000.